THE JOURNAL OF PHYSICAL CHEMISTRY A

Article

pubs.acs.org/JPCA

Structures, Hydration, and Electrical Mobilities of Bisulfate Ion−Sulfuric Acid−Ammonia/Dimethylamine Clusters: A Computational Study

Narcisse T. Tsona, Henning Henschel,* Nicolai Bork,† Ville Loukonen,‡ and Hanna Vehkamäki

Division of Atmospheric Sciences, Department of Physics, University of Helsinki, P.O. Box 64, FI-00014 University of Helsinki, Finland

Supporting Information

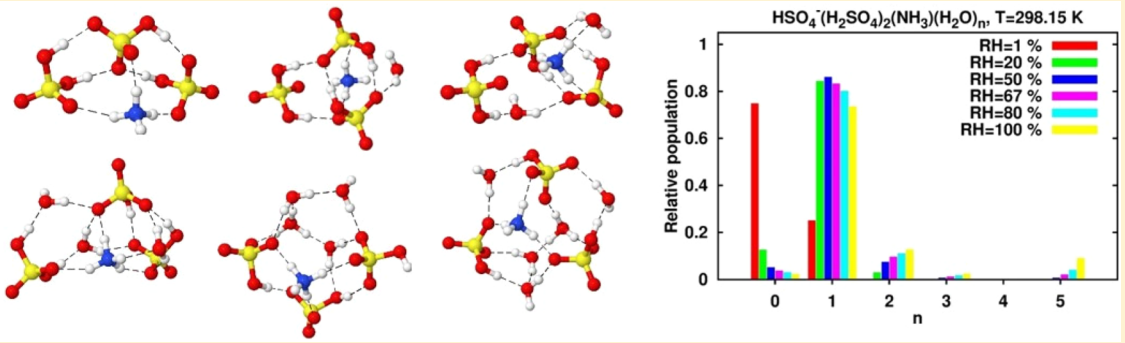

ABSTRACT: Despite the well-established role of small molecular clusters in the very first steps of atmospheric particle formation, their thermochemical data are still not completely available due to limitation of the experimental techniques to treat such small clusters. We have investigated the structures and the thermochemistry of stepwise hydration of clusters containing one bisulfate ion, sulfuric acid, base (ammonia or dimethylamine), and water molecules using quantum chemical methods. We found that water facilitates proton transfer from sulfuric acid or the bisulfate ion to the base or water molecules, and depending on the hydration level, the sulfate ion was formed in most of the base-containing clusters. The calculated hydration energies indicate that water binds more strongly to ammonia-containing clusters than to dimethylamine-containing and base-free clusters, which results in a wider hydrate distribution for ammonia-containing clusters. The electrical mobilities of all clusters were calculated using a particle dynamics model. The results indicate that the effect of humidity is negligible on the electrical mobilities of molecular clusters formed in the very first steps of atmospheric particle formation. The combination of the results of this study with those previously published on the hydration of neutral clusters by our group provides a comprehensive set of thermochemical data on neutral and negatively charged clusters containing sulfuric acid, ammonia, or dimethylamine.

INTRODUCTION

Aerosol particles are present almost everywhere in the Earth's atmosphere, and they are known to affect the climate[1,2] and to damage human health.[3,4] They are either emitted directly into the atmosphere as primary particles or formed by clustering of gaseous species.[5] The proportion of particles formed in the atmosphere constitutes a major uncertainty in predicting the net radiative forcing.[6] The detailed mechanisms driving particle formation in the atmosphere are not well-known despite the intensive research dedicated to the topic. It has been shown that sulfuric acid often plays a major role in the process,[7−9] and a number of mechanisms have been proposed to explain how sulfuric acid leads to the formation of atmospheric particles.[10] The ternary sulfuric acid−water−ammonia system has been the most studied of these mechanisms, but recently, amines and some organic compounds have been found to enhance the sulfuric acid-based particle formation rate more effectively than ammonia.[11−13]

The role of ions in atmospheric particle formation has been a controversial subject for a long time. While some studies have claimed a clear enhancement of the formation of atmospheric nanoparticles by ions,[14,15] other observations showed no clear connection between ions (formed by galactic cosmic rays and Earth's radioactive compounds) and the observed particle formation rate.[16,17] Experiments performed in the CLOUD aerosol chamber at CERN[18] demonstrated that ions do increase the particle formation rate to some extent, though not enough to explain most of the ambient observations. Nevertheless, bisulfate-containing clusters are frequently detected in the ambient atmosphere.[19] Experimental values reported on thermodynamics of some bisulfate ion−sulfuric acid clusters reveal that they have a high sulfuric acid affinity,[20] and are

Received: March 30, 2015
Revised: August 17, 2015
Published: August 24, 2015

DOI: 10.1021/acs.jpca.5b03030
J. Phys. Chem. A 2015, 119, 9670−9679

therefore favorable to cluster growth by sulfuric acid uptake. Both ammonia and dimethylamine are well-known to stabilize sulfuric acid clusters and to enhance the particle formation rate.[11,18]

Many studies investigated the effect of ammonia and dimethylamine on the hydration of sulfuric acid-containing clusters,[21−23] finding roughly similar results. Herb et al.[21] found a minor effect of one ammonia on the hydration pattern of clusters containing one bisulfate ion and sulfuric acid molecules, after considering a hydration range of three water molecules. Most recently, considering a larger hydration range (up to five water molecules), Henschel et al. studied the effect of ammonia and dimethylamine on the hydration of electrically neutral sulfuric acid clusters.[22] They found that clusters containing ammonia are less hydrated than base-free clusters at ambient conditions and that clusters containing dimethylamine are even less hydrated. To our knowledge, the study of hydration of charged clusters containing sulfuric acid has neither been extended to clusters containing more than one ammonia nor extended to any clusters containing dimethylamine molecules. However, the stability of clusters containing the bisulfate ion and sulfuric acid is known to depend on the size and number of base molecules included.[24,25]

In this study, we used quantum chemical methods to examine the structures and thermochemical properties of hydrated clusters containing one bisulfate ion, one to three sulfuric acid, and one to two base molecules ($HSO_4^-(H_2SO_4)_s(base)_b$), where s = 0−3, b = 0−2, base = ammonia or dimethylamine. We obtained hydration Gibbs free energies from quantum chemical calculations and further determined the equilibrium distributions of the different hydrates under atmospherically relevant temperature and relative humidities. The coordinates of the lowest energy configurations of all clusters were used in a particle dynamics model to calculate their electrical mobilities at 298.15 K and 1 atm.

METHODS

Geometry optimizations and vibrational frequency analysis were performed at the B3LYP/CBSB7 level of density functional theory using the Gaussian 09 package,[26] while single point energy calculations on the lowest energy B3LYP/CBSB7 optimized geometries for electronic energies correction were carried out using a wave-function-based method at the RI-CC2/aug-cc-pV(T+d)Z level using the Turbomole program.[27] The thermal contributions were calculated under the harmonic oscillator-rigid rotor approximation. The zero-point energy correction, as included in the Gibbs free energy, was calculated under this approximation as a sum of contributions from all vibrational modes of the system without a scaling factor. Vibrational modes of all clusters are listed in the Supporting Information. Some recent benchmarking studies on molecular clustering using different methods showed that, among many density functionals, B3LYP predicts reliable binding Gibbs free energies for atmospherically relevant small clusters,[28] especially when the electronic energies are corrected by the RI-CC2 module with the aug-cc-pV(T+d)Z basis set.[29,30]

Leverentz et al.[31] tested the accuracy of several computational methods against some high level coupled cluster methods assumed to yield best estimates for the binding energies of the clusters considered. From their work, it appears that the determination of binding energies of clusters with the method used in this work leads to a mean unsigned deviation of 2.52 kcal/mol from the CCSD(T)-F12a/jun-cc-pV(T+d)Z binding energies of the $(H_2SO_4)((CH_3)_2NH)$ and $(H_2SO_4)_2(NH_3)$ clusters and a mean unsigned deviation of 3.24 kcal/mol from the CCSD(T)-F12a/jun-cc-pV(T+d)Z binding energies of $(H_2SO_4)_2((CH_3)_2NH)_2$ and $(H_2SO_4)_3(NH_3)_2$. The mean unsigned deviation is known to underestimate the 95% confidence interval—the common expression of uncertainty in thermochemistry—by a factor of 2.5−3.[32] In our case, this corresponds to approximately 7−10 kcal/mol error relative to the CCSD(T)-F12a/jun-cc-pV(T+d)Z best estimates. Considering also the binding strength of water to some of these clusters, Elm and Mikkelsen[33] found that, among other methods used in their study, the method used in this work predicts Gibbs free energies in very good agreement with the best estimates from the literature.

The RI-CC2/aug-cc-pV(T+d)Z//B3LYP/CBSB7 method has repeatedly been applied to determine the Gibbs free energies used in modeling the dynamics of clusters containing sulfuric acid and ammonia or dimethylamine, with reasonable agreement with experiments (see, e.g., Kupiainen et al.,[34] Olenius et al.,[35] and Almeida et al.[11]). Moreover, we applied the same method in our earlier study on the hydration of electrically neutral clusters containing sulfuric acid and ammonia or dimethylamine.[22] Although the above-mentionned studies were mostly made on electrically neutral clusters, we believe that the RI-CC2/aug-cc-pV(T+d)Z//B3LYP/CBSB7 method will perform equally well for corresponding charged clusters, and therefore, this method is suitable for studying the clusters investigated in this work. Taking into account the electronic energy correction, the Gibbs free energy of a cluster is determined as

$$G = G_{DFT} - E_{DFT} + E_{CC} \quad (1)$$

where G_{DFT} denotes the Gibbs free energy of the cluster calculated with DFT and E_{DFT} and E_{CC} are the electronic energies calculated with DFT and RI-CC2, respectively. It should be noted that the structures were not optimized at the RI-CC2 level of theory.

A number of initial configurations were manually generated by removing one proton from a sulfuric acid molecule in our previously published structures for neutral clusters[22] and also by adding water, base, or sulfuric acid molecules to the unhydrated clusters containing one bisulfate ion and sulfuric acid published by Ortega et al.[36] This led to clusters having the $HSO_4^-(H_2SO_4)_s(base)_b(H_2O)_w$ molecular formula, where s = 0−3, b = 0−2, w = 0−5, and base = ammonia or dimethylamine. At least 25 starting configurations were generated for each of the clusters. Due to rapidly increasing computational cost with increasing cluster size, only up to two water molecules were included in clusters containing one bisulfate ion, three sufuric acids, and two base molecules.

Considering a given cluster composition, all configurations with an individual Gibbs free energy within 3 kcal/mol of the lowest free energy configuration were considered relevant, and their contribution to the free energy due to multiple configurations was calculated as[37]

$$\delta G = -RT \ln \sum_j \exp\left(-\frac{G_j}{RT}\right) \quad (2)$$

where R is the molar gas constant, T is the temperature, and G_j is the Gibbs free energy of the conformer j relative to the most stable conformer. We found that the contribution to the free

DOI: 10.1021/acs.jpca.5b03030
J. Phys. Chem. A 2015, 119, 9670−9679

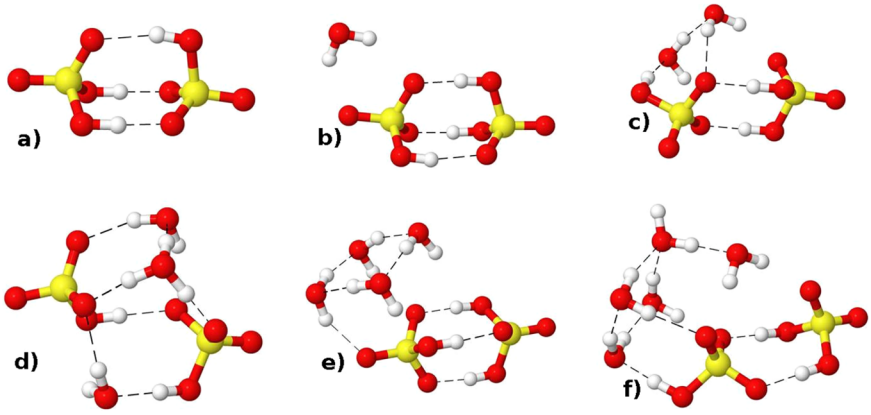

Figure 1. Most stable structures of the $HSO_4^-(H_2SO_4)(H_2O)_n$ clusters. The color coding is yellow for sulfur, red for oxygen, and white for hydrogen. The number of water molecules increases from part a where $n = 0$ to part f where $n = 5$.

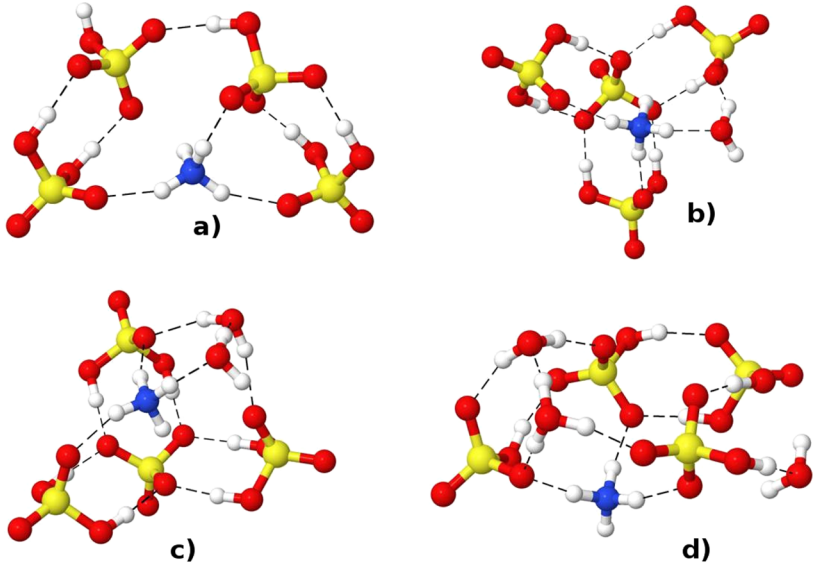

Figure 2. Most stable structures of the $HSO_4^-(H_2SO_4)_3(NH_3)(H_2O)_n$ clusters. The color coding is yellow for sulfur, blue for nitrogen, red for oxygen, and white for hydrogen. The number of water molecules increases from part a where $n = 0$ to part d where $n = 3$.

energy due to multiple configurations leads to about 0.6 kcal/mol difference relative to the lowest free energy conformer. The structures considered in eq 2 are not just any minimum but those separated by more fundamental rearrangements. As demonstrated by DePalma et al.,[38] transition state energies for such rearrangements are commonly large compared to RT, making the used approach reasonable. The Gibbs free energies of the stepwise hydration were then derived, and applying the law of mass action, we determined the equilibrium hydrate distributions of the studied clusters under atmospherically relevant temperature and relative humidities.[39] The saturation vapor pressure of water was approximated by the parametrization of Wagner and Pruss,[40] revised by Murphy and Koop.[41] The equation for calculating the equilibrium hydrate distribution is given in the Supporting Information.

Electrical mobilities and collision cross sections of ionic clusters in air were calculated using the diffuse hard sphere scattering method implemented in a particle dynamics model by Larriba and Hogan.[42,43] This method considers all collisions between gas molecules and the ion to be diffuse and thermally accommodating, and the average re-emission velocity of the gas molecules from the particle is 92% of the Maxwell distribution. Further description of this method can be found from the work of Larriba and Hogan.[42,43]

RESULTS AND DISCUSSION

Depending on the cluster compositions, two to eight configurations within 3 kcal/mol Gibbs free energy of the lowest energy configuration were obtained. The contribution due to multiple configurations was always taken into account when deriving the hydration energies and the equilibrium hydrate distributions. However, only the structures of the lowest free energy clusters are shown here and were used to calculate the electrical mobilities.

Structures. *Base-Free Clusters.* The optimized structures of base-free clusters, $HSO_4^-(H_2SO_4)_s(H_2O)_w$, were similar to those reported by Husar et al.[44] and Herb et al.[21] In tri- and higher hydrates of most cluster types with $s \geq 1$, one proton was observed to transfer from one sulfuric acid molecule to a water molecule, leading to the formation of a hydronium ion (H_3O^+) in the lowest energy configurations. Figure 1 shows the lowest energy configurations of the $HSO_4^-(H_2SO_4)$ cluster hydrates as one representative example in the base-free clusters family, while the remaining structures are shown in the

DOI: 10.1021/acs.jpca.5b03030
J. Phys. Chem. A 2015, 119, 9670−9679

Table 1. Boltzmann Averaged Gibbs Free Energy (in kcal/mol) of the Stepwise Water Addition to the Indicated Clusters, Calculated at 298.15 K[a,b]

	$n = 1$	2	3	4	5
		$HSO_4^-(H_2O)_{n-1} + H_2O \rightarrow HSO_4^-(H_2O)_n$			
this work	−4.20	−2.51	−2.45	−1.88	−1.84
CCSD(T)	−3.91	−3.32	−2.53	−1.44	−2.31
PW91	−4.58	−3.42	−2.99	−2.98	−1.38
experiment	−6.04 ± 0.44	−4.64 ± 0.50	−3.25 ± 0.25	−2.2 ± 0.44	−2.32 ± 0.56
		$HSO_4^-(H_2SO_4)(H_2O)_{n-1} + H_2O \rightarrow HSO_4^-(H_2SO_4)(H_2O)_n$			
this work	−1.05	0.05	−1.39	0.02	−1.22
PW91	−1.88	−1.10	−2.58	−0.5	0.4
experiment	−2.41 ± 1.07	−1.60 ± 0.25	−1.11 ± 0.63		
		$HSO_4^-(H_2SO_4)_2(H_2O)_{n-1} + H_2O \rightarrow HSO_4^-(H_2SO_4)_2(H_2O)_n$			
this work	−2.45	−3.28	1.11	1.51	−4.02
PW91	−1.43	−4.31	−0.68		
experiment	−1.72 ± 0.12	−2.10 ± 0.10	−1.01 ± 0.78	−1.20 ± 0.30	
		$HSO_4^-(H_2SO_4)_3(H_2O)_{n-1} + H_2O \rightarrow HSO_4^-(H_2SO_4)_3(H_2O)_n$			
this work	−4.66	−3.89	−1.96	4.53	−1.17
PW91	−3.61	−1.25	−4.75		
experiment	−2.73 ± 0.01	−1.53 ± 0.04	−1.93 ± 0.08	−1.86 ± 0.02	−2.00 ± 0.02
		$HSO_4^-(NH_3)(H_2O)_{n-1} + H_2O \rightarrow HSO_4^-(NH_3)(H_2O)_n$			
this work	−4.76	−2.56	−2.15	−0.30	−0.16
		$HSO_4^-(H_2SO_4)(NH_3)(H_2O)_{n-1} + H_2O \rightarrow HSO_4^-(H_2SO_4)(NH_3)(H_2O)_n$			
this work	−2.38	0.04	−2.23	−4.45	0.17
PW91	−1.68	−1.20	−1.44		
		$HSO_4^-(H_2SO_4)(NH_3)_2(H_2O)_{n-1} + H_2O \rightarrow HSO_4^-(H_2SO_4)(NH_3)_2(H_2O)_n$			
this work	2.21	−0.32	−6.66	3.06	−6.11
		$HSO_4^-(H_2SO_4)_2(NH_3)(H_2O)_{n-1} + H_2O \rightarrow HSO_4^-(H_2SO_4)_2(NH_3)(H_2O)_n$			
this work	−3.78	−1.25	−0.36	−1.63	−4.08
PW91	−0.50	−1.44	−2.69		
		$HSO_4^-(H_2SO_4)_2(NH_3)_2(H_2O)_{n-1} + H_2O \rightarrow HSO_4^-(H_2SO_4)_2(NH_3)_2(H_2O)_n$			
this work	1.96	−5.12	−1.39	−0.36	−5.27
		$HSO_4^-(H_2SO_4)_3(NH_3)(H_2O)_{n-1} + H_2O \rightarrow HSO_4^-(H_2SO_4)_3(NH_3)(H_2O)_n$			
this work	−5.91	−0.22	0.86		
PW91	−5.22	0.40	−1.19		
		$HSO_4^-(H_2SO_4)_3(NH_3)_2(H_2O)_{n-1} + H_2O \rightarrow HSO_4^-(H_2SO_4)_3(NH_3)_2(H_2O)_n$			
this work	−0.30	0.36			
		$HSO_4^-((CH_3)_2NH)(H_2O)_{n-1} + H_2O \rightarrow HSO_4^-((CH_3)_2NH)(H_2O)_n$			
this work	−4.56	−3.19	−2.20	−3.04	0.88
		$HSO_4^-(H_2SO_4)((CH_3)_2NH)(H_2O)_{n-1} + H_2O \rightarrow HSO_4^-(H_2SO_4)((CH_3)_2NH)(H_2O)_n$			
this work	1.89	−0.49	−3.67	−0.69	−2.23
		$HSO_4^-(H_2SO_4)((CH_3)_2NH)_2(H_2O)_{n-1} + H_2O \rightarrow HSO_4^-(H_2SO_4)((CH_3)_2NH)_2(H_2O)_n$			
this work	4.08	1.87	−8.38	−5.00	−5.67
		$HSO_4^-(H_2SO_4)_2((CH_3)_2NH)(H_2O)_{n-1} + H_2O \rightarrow HSO_4^-(H_2SO_4)_2((CH_3)_2NH)(H_2O)_n$			
this work	0.49	−3.33	4.04	−0.73	−1.57
		$HSO_4^-(H_2SO_4)_2((CH_3)_2NH)_2(H_2O)_{n-1} + H_2O \rightarrow HSO_4^-(H_2SO_4)_2((CH_3)_2NH)_2(H_2O)_n$			
this work	2.07	−3.23	2.68	−1.63	−0.19
		$HSO_4^-(H_2SO_4)_3((CH_3)_2NH)(H_2O)_{n-1} + H_2O \rightarrow HSO_4^-(H_2SO_4)_3((CH_3)_2NH)(H_2O)_n$			
this work	−7.05	6.22	4.50		
		$HSO_4^-(H_2SO_4)_3((CH_3)_2NH)_2(H_2O)_{n-1} + H_2O \rightarrow HSO_4^-(H_2SO_4)_3((CH_3)_2NH)_2(H_2O)_n$			
this work	0.65	−0.06			

[a]The values are compared to other theoretical and experimental results. [b]CCSD(T) stands for the CCSD(T)/CBS method (Husar et al.),[44] PW91 stands for the PW91PW91/6-311++G(3df,3pd) method (Herb et al., Nadykto et al.),[21,53] and experimental data are from Froyd and Lovejoy.[20]

Supporting Information. SO_4^{2-} formation was not observed in any of these cases, in accordance with Ding and Laasonen[45] and Sugawara et al.[46] who found SO_4^{2-} formation only in sulfuric acid cluster hydrates containing eight or more water molecules.

Comparing the structures of the $HSO_4^-(H_2SO_4)_s(H_2O)_w$ clusters to the corresponding electrically neutral clusters[22] (where the bisulfate ion was replaced by an intact sulfuric acid molecule), it is seen that the addition/removal of a proton does not necessarily lead to a rearrangement of molecules within the cluster. In most cases at low hydration level (0−2 water molecules), the bisulfate ion and the sulfuric acid molecules form a cluster core ($HSO_4^-(H_2SO_4)_s$) which is bound to water molecules through hydrogen bonds. At higher hydration, however, the water molecules generally act as bridges between the bisulfate ion and the sulfuric acid molecules.

DOI: 10.1021/acs.jpca.5b03030
J. Phys. Chem. A 2015, 119, 9670−9679

Ammonia-Containing Clusters. Regardless of the number of ammonia molecules involved, the ammonia-containing clusters show a tendency to form a ring structure as the number of water molecules increases. For clusters containing one ammonia molecule, one proton is transferred in most cases, with a second transfer occurring generally in tri- and higher hydrates and especially in clusters containing one bisulfate ion and at least two sulfuric acid molecules. Most cases with two proton transfers lead to the formation of SO_4^{2-} and/or H_3O^+. The H_3O^+ ion is predominantly formed in the highest hydrates (tetra- and pentahydrates) of the $HSO_4^-(H_2SO_4)_2(NH_3)$ clusters, whereas SO_4^{2-} is formed in the anhydrous cluster. Considering the dry $HSO_4^-(H_2SO_4)_2(NH_3)$ cluster, the two most stable optimized structures (one of which contains SO_4^{2-}) differ by only 0.50 kcal/mol in Gibbs free energy. The two configurations are presumably in an equilibrium where the proton is constantly transferring between the two bisulfate ions, similarly to what has been observed in sulfuric acid hydrates by Stinson et al.[47] in a path integral molecular dynamics study and in the sulfuric acid−dimethylamine monohydrate from the first-principles Born−Oppenheimer molecular dynamics study by Loukonen et al.[48] In our case, the proton transfer led to the $(HSO_4^-)_2 \leftrightarrow (SO_4^{2-})(H_2SO_4)$ isomerization within the cluster.

The clusters containing one bisulfate ion and three sulfuric acids and one ammonia showed an important feature with the SO_4^{2-} ion being formed in all of its hydrates. All the structures in which SO_4^{2-} was formed have identical configurations for the cluster core, $(H_2SO_4)_3(SO_4^{2-})(NH_4^+)$, in which the SO_4^{2-} ion is symmetrically surrounded by three H_2SO_4 molecules with the NH_4^+ ion bound to them (see Figure 2b,c).

In the systems containing two ammonia molecules, it was seen that one proton transfer occurs in the one bisulfate ion and one sulfuric acid clusters whereas two proton transfers occur in clusters containing one and two additional sulfuric acid molecules. These led to the formation of $(HSO_4^-)_2(NH_4^+)(NH_3)(H_2O)_w$- and $(HSO_4^-)_3(H_2SO_4)_{0-1}(NH_4^+)_2(H_2O)_w$-like structures for clusters containing one bisulfate ion and one sulfuric acid and those containing one bisulfate ion and two to three sulfuric acids, respectively. All structures are shown in the Supporting Information.

Dimethylamine-Containing Clusters. For clusters containing one dimethylamine molecule, there were either one or two proton transfers from one sulfuric acid or the bisulfate ion to dimethylamine or water. When there was only one proton transfer, there was no SO_4^{2-} formation, whereas transfer of a second proton would happen from the bisulfate ion, leading to the formation of SO_4^{2-}. This occurred in clusters containing one bisulfate ion and two sulfuric acids as well as in clusters containing one bisulfate ion and three sulfuric acids.

There were two proton transfers in clusters containing two dimethylamine molecules, leading to the formation of SO_4^{2-} and/or H_3O^+, depending on the degree of hydration. The formation of the SO_4^{2-} and/or H_3O^+ ions occurred already in clusters containing one bisulfate ion and one sulfuric acid, though in the unhydrated cluster and at highly hydrated conditions (four to five water molecules) only. Considering the clusters containing one bisulfate ion and two sulfuric acids and those containing one bisulfate ion and three sulfuric acids, the SO_4^{2-} ion was formed in the lowest hydrates exclusively (dry and monohydrates).

Similarly to the ammonia-containing clusters, the formation of the SO_4^{2-} ion in dimethylamine-containing clusters could not be explained by acid−base chemistry intuition. Nevertheless, it was again observed that the formation of SO_4^{2-} is favorable either at low (0−1 water molecule) or at high hydration (4−5 water molecules) levels.

Hydration Energetics and Equilibrium Hydrate Distributions. *Base-Free Clusters.* Apart from the cluster containing one bisulfate ion and one sulfuric acid molecule which shows somewhat irregular trends in Gibbs free energy of hydration, all base-free systems exhibit similar trends, with the hydration energy getting less negative with increased hydration. The numerical values for the Gibbs free energies of hydration computed at 298.15 K are presented in Table 1. We found that the hydration energies of the bisulfate ion are more negative than those of sulfuric acid molecules published in previous studies.[22,49] This is most probably the result of a strong stabilization of the negative charge on the bisulfate ion by the incoming water molecules, similarly to the effect of charge stabilization by water observed in the hydration of some oxysulfurous anions.[50,51] Our results are in good agreement with the MP2/aug-cc-pV(D+d)Z, CCSD(T)/CBS, and PW91PW91/6-311+G(3df,3pd) findings,[44,52,53] and in fairly good agreement with experiment.[20]

The clusters containing one bisulfate ion and one sulfuric acid have the weakest hydration within the base-free clusters family (see Table 1). This is likely because most energy is gained from the strong stabilization of the bisulfate ion by the sulfuric acid molecule (ΔG = −34.51 kcal/mol), as compared to the −7.89 kcal/mol binding energy between two sulfuric acid molecules.[36,54] The sign alternation of the Gibbs free energies between odd and even hydration of the $HSO_4^-(H_2SO_4)$ can be explained by inspecting the structures in Figure 1. It is seen that, while the binding of the first water molecule results in a tight structure for the monohydrate keeping the $HSO_4^-(H_2SO_4)$ configuration unchanged, the second water molecule distorts it. The addition of the third water molecule is followed by one proton transfer which likely explains the stability of the trihydrate. Upon the fourth and fifth hydration, water molecules are connected to each other to form a ring water network which is bound to the $HSO_4^-(H_2SO_4)$ core. This ring water structure seems to hinder the stability of the tetrahydrate more than the pentahydrate. The clusters containing one bisulfate ion and two or more sulfuric acid molecules are in general favorable to water addition, at least until the third hydration. The fourth hydrations are not favorable in these cases, seemingly due to the high stability of the respective trihydrates and the difficulty to incorporate the fourth water molecule in their structures. It is seen from Figure S2 in the Supporting Information that, as opposed to the trihydrate (and lower hydrates) of $HSO_4^-(H_2SO_4)_3$ where all hydrogen atoms of the water molecules are completely involved in the formation of hydrogen bonds, some water molecules in the tetrahydrate (and the pentahydrate) have dangling protons, which hinder the stability of these hydrates by not participating in the formation of hydrogen bonds.

Using the Gibbs free energies of hydration shown in Table 1, we calculated the equilibrium distributions of the $HSO_4^-(H_2SO_4)_s$ hydrates. These were explored at 252 and 298.15 K and different relative humidities (1, 20, 50, 67, 80, and 100%) chosen for atmospheric relevance and for comparability with experiments.[20] The equilibrium distribution of $HSO_4^-(H_2O)_n$ at 298.15 K shows that the bisulfate ion is extensively hydrated under most conditions (see Figure 3) and can bind one water molecule even at extremely dry conditions (at relative humidity = 1%). The equilibrium hydrate

DOI: 10.1021/acs.jpca.5b03030
J. Phys. Chem. A 2015, 119, 9670−9679

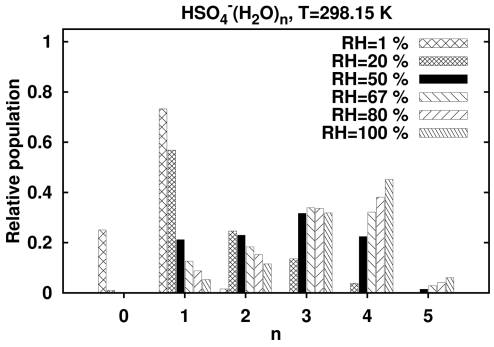

Figure 3. Equilibrium hydrate distribution of the $HSO_4^-(H_2O)_{0-5}$ clusters at 298.15 K and various relative humidities (RH).

distribution of the bisulfate ion determined by our method is in very good agreement with the high level ab initio CCSD(T)/CBS results.[44] The $HSO_4^-(H_2SO_4)$, $HSO_4^-(H_2SO_4)_2$, and $HSO4^-(H_2SO_4)_3$ clusters show narrower hydrate distributions than the bisulfate ion. They are generally dry at relative humidities below 20% while binding up to two molecules at relative humidities between 20 and 100% (related figures, i.e., Figures S14, S15, and S16 are shown in the Supporting Information). This is different from the corresponding protonated clusters whose populations are wider at all relative humidities above 10%.[22]

The major difference between the equilibrium distributions of $HSO_4^-(H_2O)_n$ at 252 and 298.15 K resides in the differences in the heights of the peaks at similar conditions. Our distributions for $HSO_4^-(H_2SO_4)_s(H_2O)_w$ clusters at 252 K agree qualitatively well with those determined experimentally by Froyd and Lovejoy[20] who produced their ionic clusters using an ion flow reactor and a quadrupole mass spectrometer for detection. At 1% relative humidity, both our method and the experiments predict $HSO_4^-(H_2O)_1$, $HSO_4^-(H_2SO_4)$, and $HSO_4^-(H_2SO_4)_2$ to be the most abundant clusters in their respective hydrate distributions. However, for the $HSO_4^-(H_2SO_4)_3(H_2O)_w$ family, we predict the most abundant cluster to be monohydrated instead of the unhydrated cluster found experimentally. For this latter case, it is however possible that this cluster, initially hydrated, loses water in the vacuum of the mass spectrometer before being detected.

For small clusters (s = 0−1), the hydrate distributions of $HSO_4^-(H_2SO_4)_s$ clusters at 67% relative humidity are also in good agreement with the experiments,[20] although we somewhat overestimate the water affinity by ca. one water molecule for large clusters (s = 2−3). For the $HSO_4^-(H_2SO_4)_2$ and $HSO_4^-(H_2SO_4)_3$ clusters, we predict the dihydrates to be the most abundant clusters in their respective hydrate distributions. Overall, our method qualitatively reproduces the $HSO_4^-(H_2SO_4)_s$ experimental hydrate distribution.

Ammonia-Containing Clusters. The hydration of ammonia-containing clusters depends strongly on the number of ammonia molecules involved. Clusters containing one ammonia molecule have more negative Gibbs free energies of hydration than base-free systems, although the average difference in the Gibbs free energy of hydration between the two cluster types rarely exceeds 1 kcal/mol. Clusters containing two ammonia molecules generally have positive Gibbs free energies at the first hydration, while negative values are obtained at the following hydration levels.

For clusters containing one ammonia molecule, hydration of the $HSO_4^-(H_2SO_4)_3(NH_3)$ cluster gives the best agreement between results reported here and those from Herb et al.[21] (with an average difference in the Gibbs free energy of hydration of ca. 0.5 kcal/mol). The first water binds strongly to $HSO_4^-(H_2SO_4)_3(NH_3)$, with ca. −5.91 kcal/mol Gibbs free energy at 298.15 K. The consequence of this highly negative value for the Gibbs free energy of first hydration of $HSO_4^-(H_2SO_4)_3(NH_3)$ is that its hydrate distribution is highly populated by monohydrates at relative humidities above 20%. This distribution is shown in Figure 4 as the representative

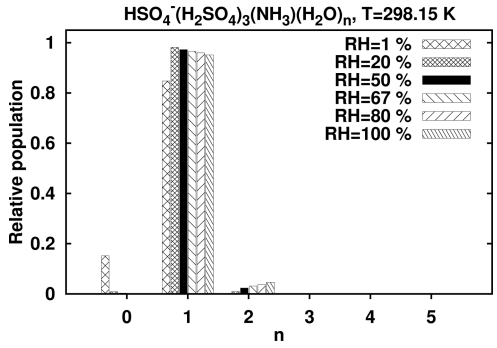

Figure 4. Equilibrium hydrate distribution of the $HSO_4^-(H_2SO_4)_3(NH_3)(H_2O)_{0-3}$ clusters at 298.15 K and various relative humidities (RH).

example of the hydrate distributions of clusters containing one ammonia molecule, while the hydrate distributions of other clusters are given in the Supporting Information.

The hydration of clusters containing two ammonia molecules is completely different from that of base-free clusters and clusters with one ammonia: the first hydration steps of clusters containing one bisulfate ion, one sulfuric acid, and two ammonia and those containing one bisulfate ion, two sulfuric acids, and two ammonia molecules are endergonic (ca. 2 kcal/mol), while the following hydrations are exergonic. The hydration of clusters containing one bisulfate ion, three sulfuric acid, and two ammonia molecules is quite weak, with −0.30 and 0.36 kcal/mol Gibbs free energy for the first and second hydration, respectively. As a consequence of this weak hydration, the clusters in this family remain almost dry at all relative humidities, with only tiny proportions of the other hydrates.

Dimethylamine-Containing Clusters. Of the clusters containing one dimethylamine molecule, those containing one bisulfate ion and one sulfuric acid and those containing one bisulfate ion and two sulfuric acid molecules have the most favorable hydration, with all but the first Gibbs free energies of hydration being negative. The first hydration step is endergonic in both cases, which results in hydrate distributions being highly populated by dry clusters at all relative humidities. Figure 5 shows the equilibrium hydrate distribution of clusters containing one bisulfate ion, two sulfuric acid, and one dimethylamine molecule as one example of clusters containing one dimethylamine molecule, and the distributions of other clusters, including those containing two dimethylamine molecules, are shown in the Supporting Information. The small amount of dihydrates in the $HSO_4^-(H_2SO_4)_2((CH_3)_2NH)$ hydrate distribution reflects the favorable addition of the second water molecule (with ΔG = −3.33 kcal/mol).

The hydration Gibbs free energies of all clusters containing two dimethylamine molecules exhibit similar trends to those in

DOI: 10.1021/acs.jpca.5b03030
J. Phys. Chem. A 2015, 119, 9670−9679

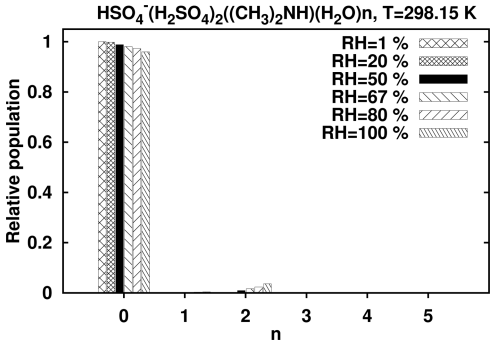

Figure 5. Equilibrium hydrate distribution of the $HSO_4^-(H_2SO_4)_2((CH_3)_2NH)(H_2O)_{0-5}$ clusters at 298.15 K and various relative humidities (RH).

clusters containing one dimethylamine molecule. In clusters containing two dimethylamine molecules, the first hydration is even more endergonic than that in clusters containing only one dimethylamine, while further hydrations are more exergonic. The hydrate distributions of these clusters are exclusively populated by the dry species at all relative humidities. The sole exception is for the $HSO_4^-(H_2SO_4)((CH_3)_2NH)_2$ cluster which is mainly populated with dry clusters at relative humidities below 20% and with pentahydrated clusters at relative humidities above 20%. The hydrate distribution of the $HSO_4^-(H_2SO_4)((CH_3)_2NH)_2$ cluster is likely a result of the stability induced by the formation of the SO_4^{2-} ion in dry and highly hydrated clusters.

In sum, regardless of the number of dimethylamine molecules involved, the hydration pattern of clusters containing dimethylamine is somewhat similar to that of clusters containing two ammonia molecules, with the first hydration being endergonic in most cases, as can be seen from Table 1. The sole case with negative energy for the first hydration is that of the $HSO_4^-(H_2SO_4)_3((CH_3)_2NH)$ cluster.

Apart from the bisulfate ion, hydrations of all other clusters investigated in this study are weaker than those of their corresponding electrically neutral forms published in our previous work.[22] It is likely that the weak binding of water to bisulfate ion-containing clusters relative to the binding to sulfuric acid-containing clusters reflects the fact that the molecules in bisulfate ion-containing clusters (which have one proton less than the corresponding neutral clusters) form less hydrogen bonds with each other and with water than the molecules in the sulfuric acid-containing clusters.

At equilibrium, while the number of water molecules bound to the $HSO_4^-(H_2SO_4)_{1-3}$ clusters at relative humidities above 10% rarely exceeds three, it is seen that at least three water molecules are always bound to the $(H_2SO_4)_{2-4}$ clusters at similar conditions.[22] Whether there is base in the cluster or not does not change the situation considerably, especially when the base is ammonia. However, in the presence of dimethylamine, the neutral clusters are still relatively highly hydrated while charged ones are mostly unhydrated at all relative humidities investigated here. The high hydration of the neutral clusters also reflects the high stability of their hydrates relative to charged clusters, and hence, the charge effect in the enhancement of new particle formation due to sulfuric acid-containing cluster hydrates might be small.

ION CLUSTER MOBILITIES

The electrical mobilities of charged particles determine their ability to move in response to an electric field and are important for size-selected measurements involving ion mobility spectrometers.[55,56] In this work, we examined the effect of humidity on the electrical mobilities of clusters calculated from the coordinates of their lowest energy configurations. Keeping in mind that clusters usually adopt many low energy configurations, the sole consideration of the lowest energy configuration in predicting the electrical mobilities is likely to be a source of uncertainties.

For clusters investigated in this study, the electrical mobilities fell in the range 1.05−3.42 $cm^2/(V\ s)$. The corresponding mobility diameters[42,55,57] fell in the range 0.52−1.11 nm, consistent with the observed range of mobility diameters for clusters formed in the very first steps of atmospheric particle formation.[58] The equation used to convert the electrical mobilities into mobility diameters is given in the Supporting Information. We found that, for all clusters, the electrical mobility decreases with increasing hydration. This is a result of the increased collision cross section of the cluster as more water molecules are bound to it. Figure 6 shows an example of the variation in electrical mobility with relative humidity for five selected ions, while the numerical values of electrical mobilities of all clusters are given in the Supporting Information. As can be seen from Figure 6, the electrical mobilities of dimethylamine-containing clusters are less sensitive to relative humidity than the mobilities of base-free clusters and ammonia-containing clusters. Due to it small size and high hygroscopicity, the bisulfate ion shows the strongest variation in electrical mobility with relative humidity. These results show that the effect of humidity is expected to be small on the electrical mobility measurements of clusters having a molecular mass above 97 Da (the molecular mass of the bisulfate ion) and particularly on those containing dimethylamine, supporting the assumption made by Jen et al.[59] Since the effect of hydration on electrical mobilities is found to be weak, the sole consideration

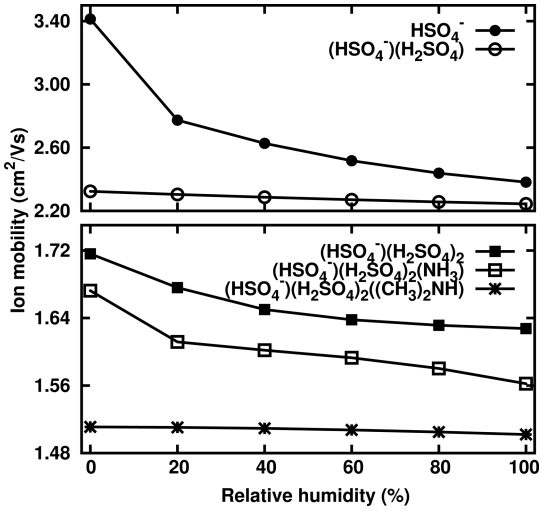

Figure 6. Variation of the electrical mobilities in air with hydration for the HSO_4^-, $HSO_4^-(H_2SO_4)$, $HSO_4^-(H_2SO_4)_2$, $HSO_4^-(H_2SO_4)_2(NH_3)$, and $HSO_4^-(H_2SO_4)_2((CH_3)_2NH)$ clusters. The molecular masses are 97, 195, 293, 310, and 338 Da, respectively. Calculations were performed at 298.15 K and 1 atm.

DOI: 10.1021/acs.jpca.5b03030
J. Phys. Chem. A 2015, 119, 9670−9679

of the lowest free energy configurations to calculate the electrical mobilities does not probably lead to a significanl error.

CONCLUSIONS

We have used ab initio calculations based on the RI-CC2/aug-cc-pV(T+d)Z//B3LYP/CBSB7 method to study atmospheric clusters consisting of one bisulfate ion, up to three sulfuric acids, up to two bases (ammonia or dimethylamine), and up to five water molecules. The structures of these clusters were determined, and the thermochemistry of their stepwise hydration was examined. In most clusters containing one bisulfate ion and at least two sulfuric acid molecules and regardless of the identity of the base molecule, the formation of the lowest energy configurations involved protons being transferred either from sulfuric acid or the bisulfate ion to the base or to water molecules. We found that, at high hydration, water facilitates the proton transfers. The formation of a sulfate ion was observed in many base-containing clusters, independently of the identity of the base molecule present.

Although most base-containing clusters exhibited positive Gibbs free energies for the first hydration, their hydration was more energetically favorable than that of base-free systems, with the exception of the bisulfate ion. Further, it was found that the hydration of ammonia-containing clusters was more favorable than that of dimethylamine-containing ones. Using the Gibbs free energy of hydration, we determined the equilibrium hydrate distributions at 252 and 298.15 K and relative humidities between 1 and 100% of all clusters studied here. Regardless of the number of bases involved, ammonia-containing clusters were more hydrated than dimethylamine-containing and base-free clusters under the investigated conditions. The combination of these results with those previously published by our group[22] provides a thorough set of thermochemical data on the hydration of neutral and negatively charged clusters containing sulfuric acid, ammonia, or dimethylamine.

The electrical mobilities of all clusters were determined from their coordinates using a particle dynamics model. The results indicate that the electrical mobilities of all but the bisulfate ion vary weakly with relative humidity. Moreover, the electrical mobilities of dimethylamine-containing clusters are almost completely insensitive to humidity. The results further indicate that at ambient conditions the effect of relative humidity is expected to be small in electrical mobility measurements of molecular clusters formed in the very first steps of atmospheric particle formation and especially for clusters containing dimethylamine.

ASSOCIATED CONTENT

Supporting Information

The Supporting Information is available free of charge on the ACS Publications website at DOI: 10.1021/acs.jpca.5b03030.

Cartesian coordinates, structures, electronic energies, entropies, enthapies, Gibbs free energies, electrical dipole moments, polarizabilities, electrical mobilities of all individual molecules/clusters in their most stable form, and hydration profiles of all clusters (PDF)

AUTHOR INFORMATION

Corresponding Author

*E-mail: henning.henschel@helsinki.fi.

Present Addresses

†N.B.: Infuser, Ole Maaløes Vej 5, bygning 779-3, 2200 Copenhagen, Denmark.

‡V.L.: Department of Applied Physics, COMP Centre of Excellence, Aalto University, P.O. Box 11100, FI-00076 Aalto, Espoo, Finland.

Notes

The authors declare no competing financial interest.

ACKNOWLEDGMENTS

The authors thank the ERC project 257360-MOCAPAF and the Academy of Finland through the centres of Excellence program (Project No. 251748) for funding and the CSC-IT Centre for Science in Espoo, Finland, for computing time. We thank Carlos Larriba who provided the IMOS package for calculating ion cluster mobilities.

REFERENCES

(1) Yu, S.; Saxena, V. K.; Zhao, Z. A Comparison of Signals of Regional Aerosol-Induced Forcing in Eastern China and the Southeastern United States. *Geophys. Res. Lett.* **2001**, *28*, 713−716.

(2) Ramanathan, V.; Crutzen, P. J.; Kiehl, J. T.; Rosenfeld, D. Aerosols, Climate, and the Hydrological Cycle. *Science* **2001**, *294*, 2119−2124.

(3) Stieb, D. M.; Judek, S.; Burnett, R. T. Meta-Analysis of Time-Series Studies of Air Pollution and Mortality: Effects of Gases and Particles and the Influence of Cause of Death, Age, and Season. *J. Air Waste Manage. Assoc.* **2002**, *52*, 470−484.

(4) Nel, A. Air Pollution-Related Illness: Effects of Particles. *Science* **2005**, *308*, 804−806.

(5) Kulmala, M. How Particles Nucleate and Grow. *Science* **2003**, *302*, 1000−1001.

(6) Stocker, T. F.; Qin, D.; Plattner, G.-K.; Tignor, M.; Allen, S. K.; Boschung, J.; Nauels, A.; Xia, Y.; Bex, V.; Midgley, P. M. *IPCC, 2013: Climate Change 2013: The Physical Science Basis. Contribution of Working Group I to the Fifth Assessment Report of the Intergovernmental Panel on Climate Change*; Cambridge University Press: Cambridge, U.K., New York, 2013; p 1535.

(7) Sihto, S.-L.; Kulmala, M.; Kerminen, V.-M.; Maso, M. D.; Petäjä, T.; Riipinen, I.; Korhonen, H.; Arnold, F.; Janson, R.; Boy, M.; et al. Atmospheric Sulphuric Acid and Aerosol Formation: Implications from Atmospheric Measurements for Nucleation and early Growth Mechanisms. *Atmos. Chem. Phys.* **2006**, *6*, 4079−4091.

(8) Riipinen, I.; Sihto, S.-L.; Kulmala, M.; Arnold, F.; Maso, M. D.; Birmili, W.; Saarnio, K.; Teinilä, K.; Kerminen, V.-M.; Laaksonen, A.; et al. Connections between Atmospheric Sulphuric Acid and New Particle Formation during QUEST III−IV Campaigns in Heidelberg and Hyytiälä. *Atmos. Chem. Phys.* **2007**, *7*, 1899−1914.

(9) Sipilä, M.; Berndt, T.; Petäjä, T.; Brus, D.; Vanhanen, J.; Stratmann, F.; Patokoski, J.; MauldinIII, R. L.; Hyvärinen, A.-P.; Lihavainen, H.; et al. The Role of Sulfuric Acid in Atmospheric Nucleation. *Science* **2010**, *327*, 1243−1246.

(10) Zhang, R.; Khalizov, A.; Wang, L.; Hu, M.; Xu, W. Nucleation and Growth of Nanoparticles in the Atmosphere. *Chem. Rev.* **2012**, *112*, 1957−2011.

(11) Almeida, J.; Schobesberger, S.; Kürten, A.; Ortega, I. K.; Kupiainen-Määttä, O.; Praplan, A. P.; Adamov, A.; Amorim, A.; Bianchi, F.; Breitenlechner, M.; et al. Molecular Understanding of Sulphuric Acid−Amine Particle Nucleation in the Atmosphere. *Nature* **2013**, *502*, 359−363.

(12) Riccobono, F.; Schobesberger, S.; Scott, C. E.; Dommen, J.; Ortega, I. K.; Rondo, L.; Almeida, J.; Amorim, A.; Bianchi, F.; Breitenlechner, M.; et al. Oxidation Products of Biogenic Emissions Contribute to Nucleation of Atmospheric Particles. *Science* **2014**, *344*, 717−721.

(13) Ehn, M.; Thornton, J. A.; Kleist, E.; Sipilä, M.; Junninen, H.; Pullinen, I.; Springer, M.; Rubach, F.; Tillmann, R.; Lee, B.; et al. A

Large Source of Low-Volatility Secondary Organic Aerosol. *Nature* **2014**, *506*, 476−479.
(14) Yu, F. From Molecular Mlusters to Nanoparticles: Second-Generation Ion-Mediated Nucleation Model. *Atmos. Chem. Phys.* **2006**, *6*, 5193−5211.
(15) Kazil, J.; Lovejoy, E. R.; Barth, M. C.; O'Brien, K. Aerosol Nucleation over Oceans and the Role of Galactic Cosmic Rays. *Atmos. Chem. Phys.* **2006**, *6*, 4905−4924.
(16) Kulmala, M.; Riipinen, I.; Sipilä, M.; Manninen, H. E.; Petäjä, T.; Junninen, H.; Maso, M. D.; Mordas, G.; Mirme, A.; Vana, M.; et al. Toward Direct Measurement of Atmospheric Nucleation. *Science* **2007**, *318*, 89−92.
(17) Kulmala, M.; Riipinen, I.; Nieminen, T.; Hulkkonen, M.; Sogacheva, L.; Manninen, H. E.; Paasonen, P.; Petäjä, T.; Maso, M. D.; Aalto, P. P.; et al. Atmospheric Data over a Solar Cycle: No Connection between Galactic Cosmic Rays and New Particle Formation. *Atmos. Chem. Phys.* **2010**, *10*, 1885−1898.
(18) Kirkby, J.; Curtius, J.; Almeida, J.; Dunne, E.; Duplissy, J.; Ehrhart, S.; Franchin, A.; Gagné, S.; Ickes, L.; Kürten, A.; et al. Role of Sulphuric Acid, Ammonia and Galactic Cosmic Rays in Atmospheric Aerosol Nucleation. *Nature* **2011**, *476*, 429−435.
(19) Ehn, M.; Junninen, H.; Petäjä, T.; Kurtén, T.; Kerminen, V.-M.; Schobesberger, S.; Manninen, H. E.; Ortega, I. K.; Vehkamäki, H.; Kulmala, M.; et al. Composition and Temporal Behavior of Ambient Ions in the Boreal Forest. *Atmos. Chem. Phys.* **2010**, *10*, 8513−8530.
(20) Froyd, K. D.; Lovejoy, E. R. Experimental Thermodynamics of Cluster Ions Composed of H_2SO_4 and H_2O. 2. Measurements and ab initio Structures of Negative Ions. *J. Phys. Chem. A* **2003**, *107*, 9812−9824.
(21) Herb, J.; Xu, Y.; Yu, F.; Nadykto, A. B. Large Hydrogen-Bonded Pre-nucleation $(HSO_4^-)(H_2SO_4)_m(H_2O)_k$ and (HSO_4^-) (NH_3)-$(H_2SO_4)_m(H_2O)_k$ Clusters in the Earths Atmosphere. *J. Phys. Chem. A* **2013**, *117*, 133−152.
(22) Henschel, H.; Navarro, J. C. A.; Yli-Juuti, T.; Kupiainen-Määttä, O.; Olenius, T.; Ortega, I. K.; Clegg, S. L.; Kurtén, T.; Riipinen, I.; Vehkamäki, H. Hydration of Atmospherically Relevant Molecular Clusters: Computational Chemistry and Classical Thermodynamics. *J. Phys. Chem. A* **2014**, *118*, 2599−2611.
(23) DePalma, J. W.; Doren, D. J.; Johnston, M. V. Formation and Growth of Molecular Clusters Containing Sulfuric Acid, Water, Ammonia, and Dimethylamine. *J. Phys. Chem. A* **2014**, *118*, 5464−5473.
(24) Bzdek, B. R.; Ridge, D. P.; Johnston, M. V. Amine Reactivity with Charged Sulfuric Acid Clusters. *Atmos. Chem. Phys.* **2011**, *11*, 8735−8743.
(25) Ortega, I. K.; Olenius, T.; Kupiainen-Määttä, O.; Loukonen, V.; Kurtén, T.; Vehkamäki, H. Electrical Charging Changes the Composition of Sulfuric Acid-Ammonia/Dimethylamine Clusters. *Atmos. Chem. Phys.* **2014**, *14*, 7995−8007.
(26) Frisch, M. J.; Trucks, G. W.; Schlegel, H. B.; Scuseria, G. E.; Robb, M. A.; Cheeseman, J. R.; Scalmani, G.; Barone, V.; Mennucci, B.; Petersson, G. A.; et al. *Gaussian 09*, revision C.01; Gaussian, Inc.: Wallingford, CT, 2010.
(27) TURBOMOLE V6.2 2010, a development of University of Karlsruhe and Forschungszentrum Karlsruhe GmbH, 1989−2007, TURBOMOLE GmbH, since 2007.
(28) Elm, J.; Bilde, M.; Mikkelsen, K. V. Assessment of Binding Energies of Atmospherically Relevant Clusters. *Phys. Chem. Chem. Phys.* **2013**, *15*, 16442−16445.
(29) Bork, N.; Du, L.; Kjaergaard, H. G. Identification and Characterization of the HCl-DMS Gas Phase Molecular Complex via Infrared Spectroscopy and Electronic Structure Calculations. *J. Phys. Chem. A* **2014**, *118*, 1384−1389.
(30) Bork, N.; Du, L.; Reiman, H.; Kurtén, T.; Kjaergaard, H. G. Benchmarking Ab Initio Binding Energies of Hydrogen-Bonded Molecular Clusters Based on FTIR Spectroscopy. *J. Phys. Chem. A* **2014**, *118*, 5316−5322.
(31) Leverentz, H. R.; Siepmann, J. I.; Truhlar, D. G.; Loukonen, V.; Vehkamäki, H. Energetics of Atmospherically Implicated Clusters Made of Sulfuric Acid, Ammonia, and Dimethyl Amine. *J. Phys. Chem. A* **2013**, *117*, 3819−3825.
(32) Ruscic, B. Uncertainty Quantification in Thermochemistry, Benchmarking Electronic Structure Computations, and Active Thermochemical Tables. *Int. J. Quantum Chem.* **2014**, *114*, 1097−1101.
(33) Elm, J.; Mikkelsen, K. V. Computational Approaches for Efficiently Modelling of Small Atmospheric Clusters. *Chem. Phys. Lett.* **2014**, *615*, 26−29.
(34) Kupiainen, O.; Ortega, I. K.; Kurtén, T.; Vehkamäki, H. Amine Substitution into Sulfuric Acid - Ammonia Clusters. *Atmos. Chem. Phys.* **2012**, *12*, 3591−3599.
(35) Olenius, T.; Kupiainen-Määttä, O.; Ortega, I. K.; Kurtén, T.; Vehkamäki, H. Free Energy Barrier in the Growth of Sulfuric Acid-Ammonia and Sulfuric Acid-Dimethylamine Clusters. *J. Chem. Phys.* **2013**, *139*, 084312-1−084312-12.
(36) Ortega, I. K.; Kurtén, T.; Vehkamäki, H.; Kulmala, M. The Role of Ammonia in Sulfuric Acid Ion Induced Nucleation. *Atmos. Chem. Phys.* **2008**, *8*, 2859−2867.
(37) Ho, J.; Coote, M. L.; Cramer, C. J.; Truhlar, D. G. Theoretical Calculation of Reduction Potentials. In *Organic Electrochemistry*, 5th ed.; Hammerich, O., Speiser, B., Eds.: CRC Press: Boca Raton, FL, 2015.
(38) DePalma, J. W.; Bzdek, B. R.; Ridge, D. P.; Johnston, M. V. Activation Barriers in the Growth of Molecular Clusters Derived from Sulfuric Acid, and Ammonia. *J. Phys. Chem. A* **2014**, *118*, 11547−11554.
(39) Noppel, M.; Vehkamäki, H.; Kulmala, M. An Improved Model for Hydrate Formation in Sulfuric Acid-Water Nucleation. *J. Chem. Phys.* **2002**, *116*, 218−228.
(40) Wagner, W.; Pruss, A. International Equations for the Saturation Properties of Ordinary Water Substance. Revised According to the International Temperature Scale of 1990. Addendum to J. Phys. Chem. Ref. Data 16, 893 (1987). *J. Phys. Chem. Ref. Data* **1993**, *22*, 783−787.
(41) Murphy, D. M.; Koop, T. Review of the Vapour Pressures of Ice and Supercooled Water for Atmospheric Applications. *Q. J. R. Meteorol. Soc.* **2005**, *131*, 1539−1565.
(42) Larriba, C.; Hogan, C. J. Ion Mobilities in Diatomic Gases: Measurement versus Prediction with Non-Specular Scattering Models. *J. Phys. Chem. A* **2013**, *117*, 3887−3901.
(43) Larriba, C.; Hogan, C. J. Free Molecular Collision Cross Section Calculation Methods for Nanoparticles and Complex Ions with Energy Accommodation. *J. Comput. Phys.* **2013**, *251*, 344−363.
(44) Husar, D. E.; Temelso, B.; Ashworth, A. L.; Shields, G. C. Hydration of the Bisulfate Ion: Atmospheric Implications. *J. Phys. Chem. A* **2012**, *116*, 5151−5163.
(45) Ding, C.-G.; Laasonen, K. Partially and Fully Deprotonated Sulfuric Acid in $H_2SO_4(H_2O)_n$ (n = 6−9) Clusters. *Chem. Phys. Lett.* **2004**, *390*, 307−313.
(46) Sugawara, S.; Yoshikawa, T.; Takayanagi, T. Quantum Proton Transfer in Hydrated Sulfuric Acid Clusters: A Perspective from Semiempirical Path Integral Simulations. *J. Phys. Chem. A* **2011**, *115*, 11486−11494.
(47) Stinson, J. L.; Kathmann, S. M.; Ford, I. J. Investigating the Ssignificance of Zero-Point Motion in Small Molecular Clusters of Sulfuric Acid and Water. *J. Chem. Phys.* **2014**, *140*, 024306-1−024306-6.
(48) Loukonen, V.; Bork, N.; Vehkamäki, H. From Collisions to Clusters: First Steps of Sulphuric Acid Nanocluster Formation Dynamics. *Mol. Phys.* **2014**, *112*, 1979−1986.
(49) Temelso, B.; Morrell, T. E.; Shields, R. M.; Allodi, M. A.; Wood, E. K.; Kirschner, K. N.; Castonguay, T. C.; Archer, K. A.; Shields, G. C. Quantum Mechanical Study of Sulfuric Acid Hydration: Atmospheric Implications. *J. Phys. Chem. A* **2012**, *116*, 2209−2224.
(50) Tsona, T. N.; Bork, N.; Vehkamäki, H. On the Gas-Phase Reaction between SO_2 and $O_2^-(H_2O)_{0-3}$ Clusters - an ab initio Study. *Phys. Chem. Chem. Phys.* **2014**, *16*, 5987−5992.

DOI: 10.1021/acs.jpca.5b03030
J. Phys. Chem. A 2015, 119, 9670−9679

(51) Tsona, T. N.; Bork, N.; Vehkamäki, H. Exploring the Chemical Fate of the Sulfate Radical Anion by Reaction with Sulfur Dioxide in the Gas Phase. *Atmos. Chem. Phys.* **2015**, *15*, 495−503.
(52) Kurtén, T.; Noppel, M.; Vehkamäki, H.; Salonen, M.; Kulmala, M. Quantum Chemical Studies of Hydrate Formation of H_2SO_4 and HSO_4^-. *Boreal Env. Res.* **2007**, *12*, 431−453.
(53) Nadykto, A. B.; Yu, F.; Herb, J. Theoretical Analysis of the Gas-Phase Hydration of Common Atmospheric Pre-Nucleation (HSO_4^-)-$(H_2O)_n$ and $(H_3O^+)(H_2SO_4)(H_2O)_n$ Cluster Ions. *Chem. Phys.* **2009**, *360*, 67−73.
(54) Ortega, I. K.; Kupiainen, O.; Kurtén, T.; Olenius, T.; Wilkman, O.; McGrath, M. J.; Loukonen, V.; Vehkamäki, H. From Quantum Chemical Formation Free Energies to Evaporation Rates. *Atmos. Chem. Phys.* **2012**, *12*, 225−235.
(55) de la Mora, J. F.; de Luan, L.; Thilo, E.; Rosell, J. Differential Mobility Analysis of Molecular Ions and Nanometer Particles. *TrAC, Trends Anal. Chem.* **1998**, *17*, 328−339.
(56) Ehn, M.; Junninen, H.; Schobesberger, S.; Manninen, H.; Franchin, A.; Sipilä, M.; Petäjä, T.; Kerminen, V.-M.; Tammet, H.; Mirme, A.; et al. An Instrumental Comparison of Mobility and Mass Measurements of Atmospheric Small Ions. *Aerosol Sci. Technol.* **2011**, *45*, 522−532.
(57) Bohrer, B. C.; Merenbloom, S. I.; Koeniger, S. L.; Hilderbrand, A. E.; Clemmer, D. E. Biomolecule Analysis by Ion Mobility Spectrometry. *Annu. Rev. Anal. Chem.* **2008**, *1*, 293−327.
(58) Kulmala, M.; Kontkanen, J.; Junninen, H.; Lehtipalo, K.; Manninen, H. E.; Nieminen, T.; Petäjä, T.; Sipilä, M.; Schobesberger, S.; Rantala, P.; et al. Direct Observations of Atmospheric Aerosol Nucleation. *Science* **2013**, *339*, 943−946.
(59) Jen, C. N.; Hanson, D. R.; McMurry, P. H. Toward Reconciling Measurements of Atmospherically Relevant Clusters by Chemical Ionization Mass Spectrometry and Mobility Classification/Vapor Condensation. *Aerosol Sci. Technol.* **2015**, *49*, i−iii.

DOI: 10.1021/acs.jpca.5b03030
J. Phys. Chem. A 2015, 119, 9670−9679